Wetlands (2013) 33:141–155
DOI 10.1007/s13157-012-0359-8

ARTICLE

Topographic Metrics for Improved Mapping of Forested Wetlands

Megan Lang · Greg McCarty · Robert Oesterling · In-Young Yeo

Received: 12 January 2012 / Accepted: 23 November 2012 / Published online: 12 December 2012

Abstract We investigated the predictive strength of forested wetland maps produced using digital elevation models (DEMs) derived from Light Detection and Ranging (LiDAR) data and multiple topographic metrics, including multiple topographic wetness indices (TWIs), a TWI enhanced to incorporate information on water outlets, normalized relief, and hybrid TWI/relief in the Coastal Plain of Maryland. LiDAR DEM based wetland maps were compared to maps of inundation and existing wetland maps. TWIs based on the most distributed FD8 (8 cells) and somewhat distributed D∞ (1–2 cells) flow routing algorithms were better correlated with inundation than a TWI based on a non-distributed D8 (1 cell) flow routing algorithm, but D∞ TWI class boundaries appeared artificial. The enhanced FD8 TWI provided good prediction of wetland location but could not predict periodicity of inundation. Normalized relief provided good prediction of inundation periodicity but was less able to map wetland boundaries. A hybrid of these metrics provided good measurement of wetland location and inundation periodicity. Wetland maps based on topographic metrics included areas of flooded forest that were similar to an aerial photography based wetland map. These results indicate that LiDAR based topographic metrics have potential to improve accuracy and automation of wetland mapping.

Keywords Hydroperiod · Hydropattern · Inundation · Relief · Topographic wetness index · Wetland mapping

M. Lang (✉)
USDA Forest Service, Northern Research Station,
10300 Baltimore Ave., Bldg 007, Rm 104,
Beltsville, MD 20705, USA
e-mail: mwlang@fs.fed.us

G. McCarty
USDA Agricultural Research Service,
Beltsville Agricultural Research Center,
Hydrology and Remote Sensing Laboratory,
10300 Baltimore Ave., Bldg 007, Rm 104,
Beltsville, MD 20705, USA

R. Oesterling · I.-Y. Yeo
Department of Geography, University of Maryland,
2182 LeFrak Hall,
College Park, MD 20742, USA

Introduction

To best preserve wetlands and associated ecosystem services in the face of climate and land-use change, wetlands must be monitored routinely. Wetland mapping is an essential part of this monitoring program. Remote observation of wetlands is necessary because they are often difficult to access on the ground, and on-site mapping at the landscape scale is cost-prohibitive. One of the most common wetland mapping methods uses optical images, such as aerial photography, in conjunction with field data. The U.S. Fish and Wildlife Service National Wetland Inventory (NWI) is one of the earliest and most commonly relied upon U.S. wetland maps. NWI maps are primarily produced using aerial photographs, photointerpretation techniques, and field verification (Tiner 1990). Although great care has been taken in the production of these maps and they are relied upon by numerous scientists and managers (Kudray and Gale 2000), challenges to the cartographic process remain. This is especially true in forested areas where errors vary widely but can be substantial (Stolt and Baker 1995; Kudray and Gale 2000). Furthermore, the photointerpretation process is not automated, and is therefore time and resource intensive and somewhat subjective.

One of the most difficult types of wetlands to map is palustrine forested wetlands (Tiner 1990). This is especially true in areas of low topographic relief, such as the outer Coastal Plain of the Mid-Atlantic U.S. Palustrine forested

wetlands are difficult to map because the forest canopy often prevents viewing of the ground's surface. Furthermore, trees found in this type of wetland are often identical or spectrally similar to those found in upland forests, and the expression of wetland hydrology is often intermittent. Moreover, relatively small variations in topography are capable of forming these types of wetlands. As a result, all forested wetlands, but especially smaller, drier wetlands, are difficult to detect.

Recently developed remote sensing technologies and techniques have the potential to improve the detail and reliability of wetland maps. One of these relatively new and rapidly developing technologies is discrete point return imaging light detection and ranging (LiDAR). LiDAR data can be used to calculate precise x,y,z locations by recording the amount of time it takes for an emitted pulse, or a portion of that pulse, to return to the sensor (Vierling et al. 2008). LiDAR x,y,z points can be used to make digital elevation models (DEMs). Although topographic information is commonly available for the United States, the spatial resolution of these data is often not sufficient for wetland identification, especially in areas of subtle topographic change, like the Mid-Atlantic Coastal Plain. In general, conventional, non-LiDAR derived DEMs have much coarser vertical accuracies (1 – 10 m) than those derived from LiDAR (~ 10 cm; Coren and Sterzai 2006). LiDAR derived DEMs also have relatively fine horizontal resolution (~ 100 cm; Coren and Sterzai 2006). While return time provides information on location, LiDAR intensity, or the strength of the returned LiDAR signal relative to the amount of energy transmitted by the sensor per laser pulse (Chust et al. 2008), provides information regarding the identity of materials off which the LiDAR signal reflects before returning to the sensor.

LiDAR-derived DEMs are often used to derive primary topographic metrics, such as slope and aspect, and compound or secondary metrics, which are based on the relationship between multiple primary metrics. Secondary topographic metrics, like topographic wetness indices, have been used to determine the spatial distribution of key wetland processes (Moore et al. 1991; Bohner and Selige 2006), such as soil saturation. The topographic wetness index (TWI), which is based on slope and contributing area, is expressed as $\ln(\alpha/\tan\beta)$, where α is the upslope contributing area per unit contour and $\tan\beta$ is the local topographic gradient (Beven and Kirkby 1979). Soil transmissivity is assumed to be constant (Moore et al. 1991). Areas with higher topographic wetness index values are likely to be wetter relative to areas with lower values.

The TWI is commonly used to characterize soils (e.g., Bohner and Selige 2006), but can also be used to map vegetation (Kopecky and Cizkova 2010). However, the use of TWI to map wetlands has been limited (Rohde and Seibert 1999; Curie et al. 2007; Murphy et al. 2009 [index similar to TWI]; Walker et al. 2012). Furthermore, although a number of studies have tested the behavior of flow routing algorithms in generalized landscapes, few studies have tested the influence of flow routing algorithms on TWI performance using spatially distributed reference data (Sorensen et al. 2006) or investigated algorithm performance in areas of low topographic relief where wetlands are most common. Wilson et al. (2007) call for the investigation of different flow routing algorithms for different landscapes (i.e., flat) and applications.

When using raster DEMs to generate inputs for the TWI, β is usually measured using the same procedure (i.e., a 3 kernel area centered on the pixel of interest; Bohner et al. 2001). However, the procedures used to generate α vary considerably with different flow routing algorithms. These flow routing algorithms are often divided into single and multiple flow routing algorithms with single flow routing algorithms routing water from a target cell to one adjoining cell and multiple flow routing algorithms routing water to multiple adjoining cells, thus allowing for more distributed flow (Arnold 2010; Kopecky and Cizkova 2010). The D8 flow routing algorithm (O'Callaghan and Mark 1984) is a single flow routing algorithm that determines which of eight directions water should flow (e.g., north, northeast, east, etc.) based on the steepest downslope neighboring pixel. This is the algorithm most commonly used by GIS programs (Arnold 2010; Kopecky and Cizkova 2010), including ArcGIS (ESRI; Redlands, California). A number of multiple flow routing algorithms have been proposed which distribute water to neighboring cells based on more complex decision rules. These algorithms include the deterministic infinity ($D\infty$) algorithm proposed by Tarboton (1997) and FD8 algorithm proposed by multiple authors including Freeman (1991). The $D\infty$ algorithm routes water to one or two neighboring cells determined by greatest slope. If the flow angle of greatest descent leads directly to a single pixel, water is routed to that pixel but if the angle is situated between pixels water is proportioned between the two pixels based on how close the angle is to the adjoining pixels (Tarboton 1997). The FD8 algorithm routes water to all eight neighboring cells with the amount of flow determined by slope, with steeper slopes between the target and neighboring cells causing more water to be routed than shallower slopes (Freeman 1991).

The strong potential of LiDAR for ecologic applications has been recognized by both scientists and managers (Lefsky et al. 2002), but the methods necessary to apply these data for improved wetland mapping have not been fully explored. The research described herein supports the development of more rapid and reliable operational wetland mapping within forested environments. We investigated the predictive strength of forested wetland maps produced using DEMs derived from LiDAR and multiple topographic metrics,

including previously published and newly established metrics, in Maryland's Coastal Plain. LiDAR based mapping products were compared to highly accurate maps of inundation derived from LiDAR intensity (Lang and McCarty 2009) and the most accurate wetland map currently available for the study site.

Methods

Study Site

The 33 km^2 study site is located within the Choptank River Watershed (Fig. 1), and focused primarily on the 690 km^2 Tuckahoe Creek Watershed, a sub-watershed of the Choptank. The Choptank River, a major tributary of the Chesapeake Bay, originates in Kent County, Delaware and flows southwest towards its outlet near Cambridge, Maryland. The 1,756 km^2 Choptank River Watershed is located on the Delmarva Peninsula within the Coastal Plain Physiographic Province. The area is characterized by a humid, temperate climate with average annual precipitation of 120 cm/yr (Ator et al. 2005). Approximately 50 % of annual precipitation is lost to the atmosphere via evapotranspiration while the remainder recharges ground water or enters streams via surface flow (Ator et al. 2005). The area is relatively flat (max elevation <30 m above sea level) and land cover is dominated by agriculture (~60 %) with smaller amounts of forest (33 %) and urban/suburban area (7 %; McCarty et al. 2008).

A significant percent of forested area within the Choptank River Watershed is wetland. The primary soil types within forested areas at the study site are Hammonton-Fallsington-Corsica complex (predominantly moderately well drained), Corsica mucky loam (predominantly very poorly drained), and Fallsington sandy loam (predominantly poorly drained) in order from most to least common. The spatial distribution of hydric soils across the study area can be seen in Fig. 2. The primary types of wetlands found within the study area are wetland depressions (e.g., Delmarva bays) and wetland flats, with smaller amounts of riparian wetlands. Most wetlands are inundated or saturated for a relatively short period of time within the growing season, usually in early spring after snowmelt and before leaf-out. The period of maximum hydrologic expression (i.e., highest groundwater levels and most area inundated) varies with fluctuations in weather, but is typically in or around March when evapotranspiration has been relatively low for the longest period of time and before evapotranspiration increases markedly with rising temperatures and leaf-out. Although a significant amount of forested wetlands remain, many have been lost to drainage or fill.

Geospatial Data

The topographic metrics were developed using a DEM derived from LiDAR data that were collected when very little flooding of any type was present in wetlands. Data

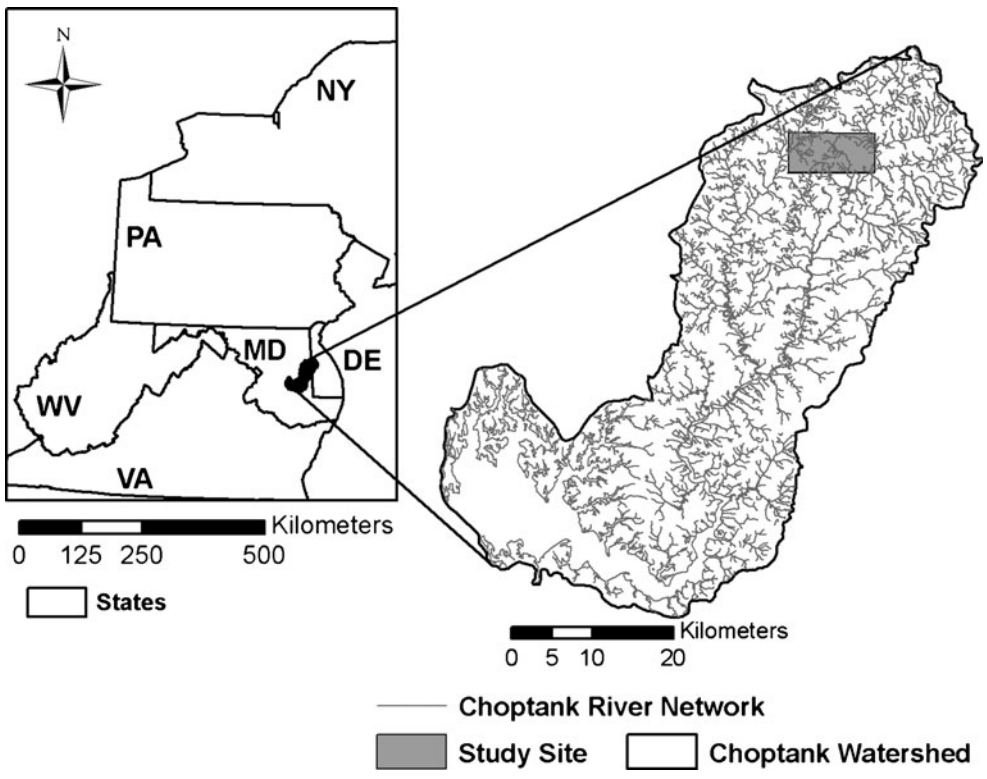

Fig. 1 The Tuckahoe Creek Watershed which is located in the headwaters of the Choptank River Network, Maryland

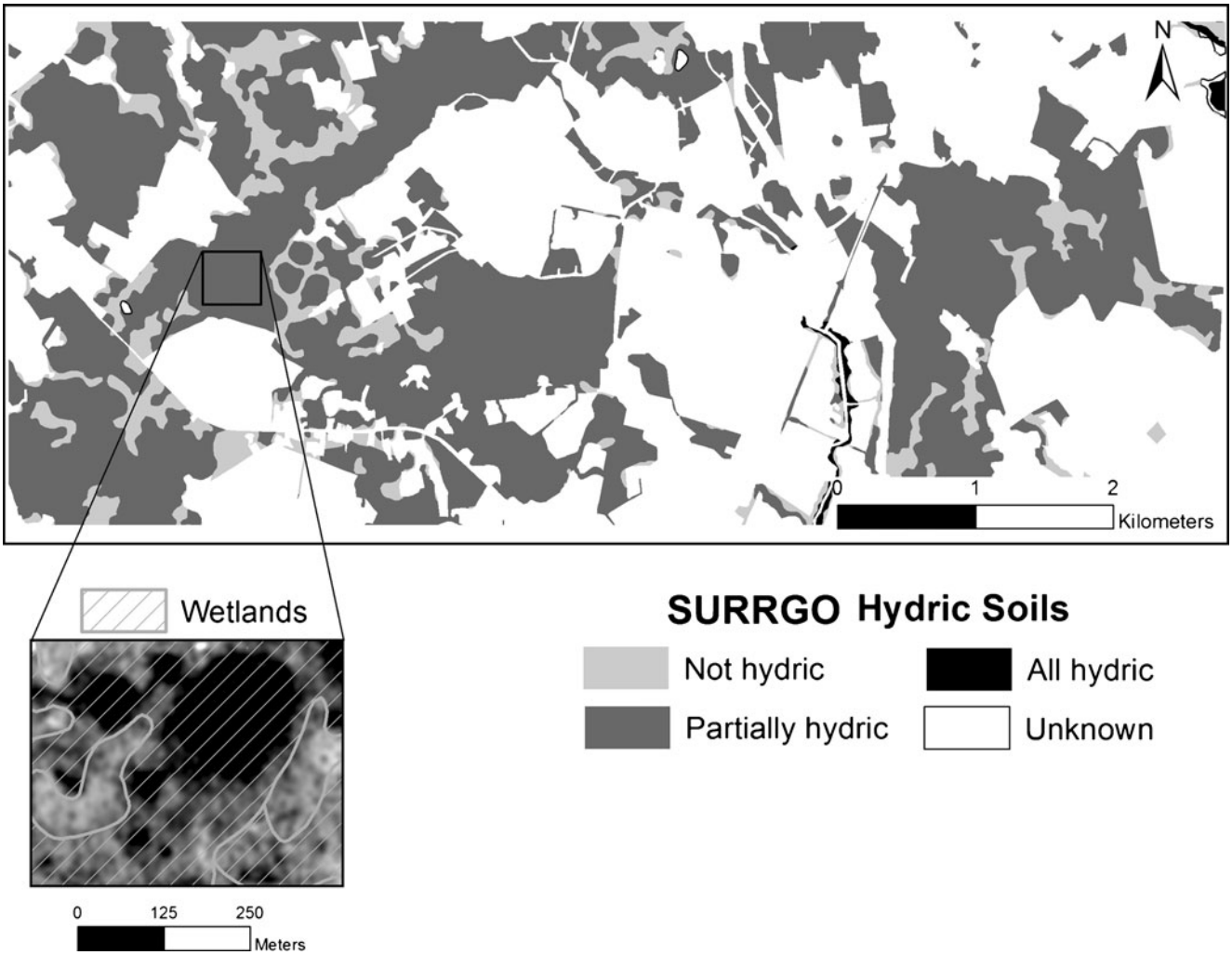

Fig. 2 The spatial distribution of hydric soils, partially hydric soils, and non-hydric soils across the study area. Note that wetland boundaries as mapped by MD DNR are more spatially explicit than hydric soils boundaries within the selected forested area. This is generally true across the study area

were collected using a Leica ALS50-II sensor on December 24, 2007 using a scan angle of +/− 25° at a height of 1,829 m above the Earth's surface with a pulse rate of 126,000 Hz and scan frequency of 50 Hz. Raw data were converted to LAS files, a commonly used LiDAR data exchange format, containing x, y, z, and intensity data. Bare earth points (i.e., points originating from the Earth's surface instead of structural components above the Earth's surface [e.g., trees]) were classified by the data provider using Terrascan (v. 7.0; Terrasolid Limited, Helsinki, Finland) and Fugro EarthData proprietary software. The data were validated using over 100 precision GPS points collected at areas of stable elevation (e.g., road intersections) using a Trimble RTK 4700 GPS/base station combination and a surveyed benchmark provided by the Maryland State Highway Administration. The end product had a vertical accuracy of ≤ 0.15 m and a pulse density of~2.8 pts/m^2 (~ 0.35 m post spacing). It should be noted that vertical accuracy is likely to be somewhat reduced within forested areas, relative to areas without vegetation or other vertical structures that can obscure the ground's surface (Hogg and Holland 2008).

In order to help gauge relative predicative strength, LiDAR intensity data were collected over the study area on March 27, 2007 and March 24, 2009. These dates were selected to represent both average (2007) and moderate drought (2009) conditions according to the Palmer Z Index as calculated over a 3 month time period (National Oceanic and Atmospheric Administration National Climate Data Center: http://cdo.ncdc.noaa.gov). The dates also correspond with the approximate average period of maximum hydrologic expression and were at the beginning of the local growing season as it relates to the definition of wetlands (last −2.22° C or lower freeze at the 50 % probability level for Dover, Delaware is March 28; National Oceanic and Atmospheric Administration National Climate Data Center: http://cdo.ncdc.noaa.gov). Precipitation did not occur for at least 4 days before the March 27,

2007 and March 24, 2009 acquisitions. Data were collected using an Optech ALTM 3100 LiDAR sensor on March 27, 2007 with a scan angle of +/−20° at a height of 610 m above the Earth's surface with a pulse rate of 100,000 Hz and a scan frequency of 50 Hz. Data were collected on March 24, 2009 using the same sensor with a scan angle of +/−10° at a height of 610 m above the Earth's surface with a pulse rate of 100,000 Hz and scan frequency of 70 Hz. LiDAR points were validated using the same 100 precision GPS points described above. Raw data were converted to LAS files containing x, y, z, and intensity data and bare earth points were classified by the data provider using Terrascan v 7.0 software. The resultant data had a vertical accuracy of ≤ 0.15 m and an average point density of ~2.5 pts/m^2 (0.40 m post spacing) or ~11 pts/m^2 (0.09 m post spacing), for the 2007 and 2009 datasets, respectively. The ALTM 3100 sensor was coupled with a digital camera to capture coincident 12 cm spatial resolution aerial photography in the near-infrared (720–920 nm), red (600–720), and green (510–600) bands.

The Maryland Department of Natural Resources (MD DNR) wetland map was the most current fine resolution (1:12,000) wetland map available for the study area. The MD DNR wetland map was generated using the same classification system (i.e., Cowardin et al. [1979]) and basic method utilized to create NWI maps except that the MD DNR wetland map was based on more recently collected, finer resolution aerial photographs (late 1980s – early 1990s; metadata located at: ftp://dnrftp.dnr.state.md.us/public/SpatialData/Wetlands/WetlandsDNR/County/dnrwet.htm; last accessed July 2012).

Analysis

The methods used to preprocess the DEM and create the topographic metric based wetland maps are described below, and summarized in Fig. 3.

LiDAR Preprocessing

LP360 software (v. 2.0; QCoherent Software, LLC; Colorado Springs, CO) was used to import tiled bare earth LAS files. Bridges, and other obstructions to modeled two-dimensional flow that can lead to inaccurate water routing, were manually identified and LP360 software was then used to lower the December 24, 2007 bare earth point elevations to the level of flowing water at those locations. Although such impediments to modeled two dimensional flow were rare within the forested study site, this was done to eliminate the potential effect of these impediments on study results. Inverse distance weighted (IDW) interpolation was used to produce a 3 m gridded DEM for the December date and 1 m intensity images for the March dates (March 27, 2007 and March 24, 2009). Similar to other interpolation methods, the use of IDW and the nature of LiDAR data can lead to local variation in values and filtering is used to suppress sudden increases or decreases in pixel values that may result from noise (Yu et al. 2002). The DEM was iteratively filtered using a 3 kernel and then a 9 kernel low pass filter. The early spring intensity images were passed through an enhanced Lee filter (Lopes et al. 1990) five times with increasing kernel sizes of 3 (twice), 5, 7, and 9.

Topographic Metrics

The filtered 3 m DEM, collected on December 24, 2007, was used to parameterize three different topographic wetness index algorithms including those based on D8, D∞, and FD8 flow routing algorithms. Sinks were not filled before running the flow routing algorithms. The D8 flow routing algorithm was calculated using the System for Automated Geoscientific Analysis (SAGA) v. 2.0.8, free open source software designed for the analysis of spatial data (D8 flow analysis module;

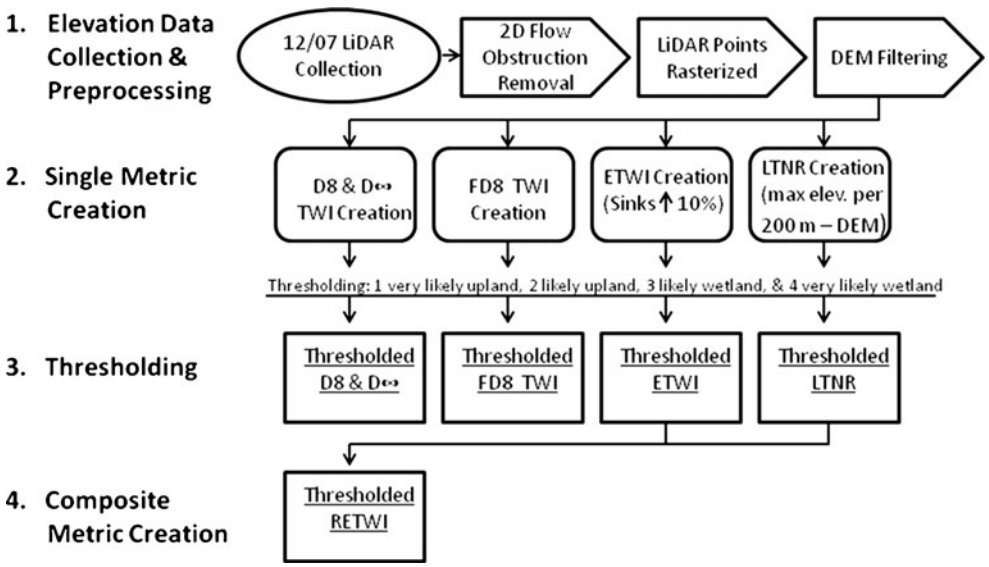

Fig. 3 A flow-chart illustrating DEM preprocessing and topographic metric creation. Initial data are indicated with *ovals*, processing steps are indicated by *pentagons*, preliminary products are indicate by *rounded rectangles*, and final products, which were compared with in situ data, are indicated by *rectangles*

Conrad 2006) and the resultant data were used to calculate the D8 TWI in ArcGIS (v. 9.3) according to the equation developed by Beven and Kirkby (1979). The FD8 TWI was calculated using the SAGA Wetness Index module (Bohner and Selige 2006). Terrain Analysis Using Digital Elevation Models (TAUDEM) v. 5.0 software was used to calculate specific catchment area based on the D∞ algorithm and the resultant dataset was used in ArcGIS to calculate a TWI according to the equation developed by Beven and Kirkby (1979).

A local terrain normalized relief (LTNR) map was created and existing topographic metrics were modified to better represent drivers of wetland water budgets (i.e., water inputs and outputs). To create the LTNR map (Fig. 4a), ArcGIS was used to create a continuous surface of maximum elevation per 200 m^2 area. The original (unfiltered) 3 m DEM was filtered twice using a 3 kernel low pass filter and the maximum elevation dataset was subtracted from the filtered 3 m DEM to create the LTNR map. An enhanced topographic wetness index (ETWI) was created (Fig. 4b) by increasing FD8 based wetness index values within depressions (i.e., pits or sinks) by 10 %. The range of pixel values within each topographic metric was assessed by noting the highest and lowest values included within 99 % of all pixels. The highest and lowest 0.5 % of pixel values were excluded to reduce potential error which might bias the range.

The continuous values within all LiDAR derived topographic metrics (i.e., D8, D∞, FD8, LTNR, and ETWI) were then thresholded to create four classes: 1) very likely to be upland, 2) likely to be upland, 3) likely to be wetland, and 4) very likely to be wetland. The thresholds were created qualitatively based on best professional judgment and review of ancillary data including multiple dates of leaf-off aerial photography and existing wetland maps including the MD DNR wetland map and the NWI (all datasets that are commonly available throughout the US). Normalizing the LTNR and ETWI through thresholding allowed the LTNR and ETWI products to be added together to create the relief enhanced topographic wetness index (RETWI; Fig. 4c), with values from 2 to 8 (higher values indicating greater likelihood of wetlands; e.g., 8 means LTNR and ETWI agree area is very likely to be a wetland).

Predictive Strength

Topographic metric based wetland maps were compared with LiDAR intensity derived maps of inundation created for March 27, 2007 (average weather conditions) and March 24, 2009 (drought conditions) to gauge relative predictive strength of products and potential of mapping techniques to support future operational wetland mapping efforts. The

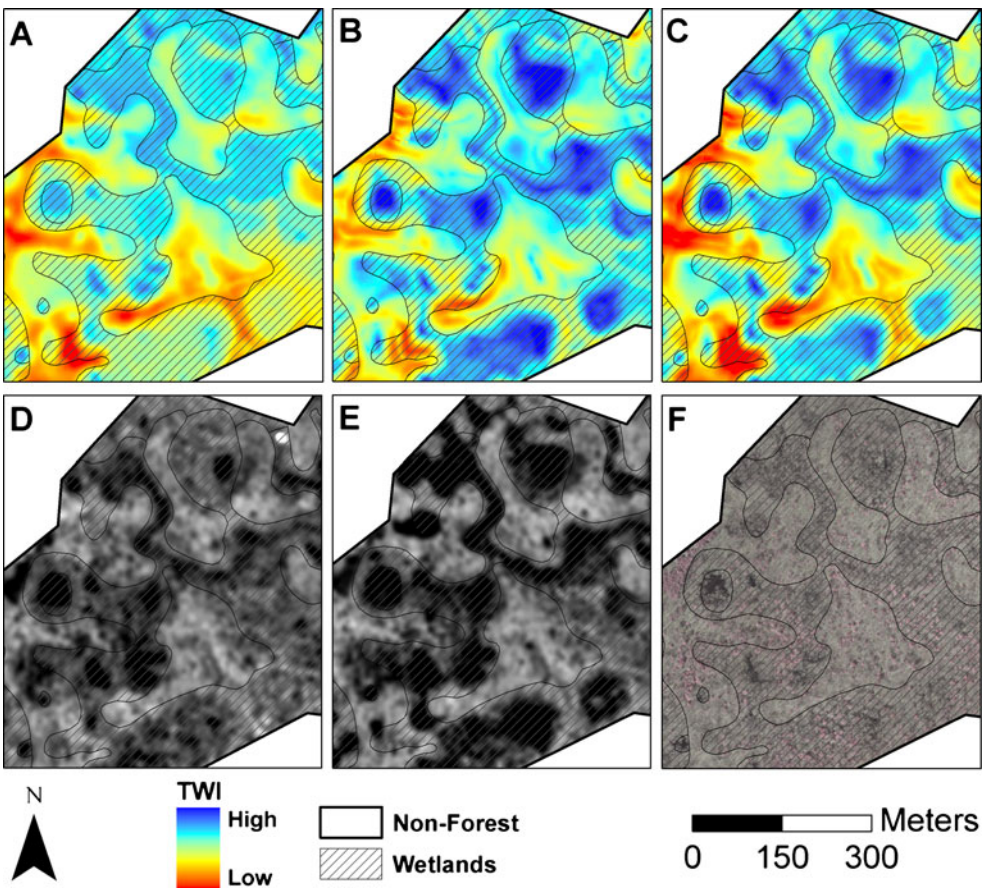

Fig. 4 Topographic index products including the local terrain normalized relief (**a**), enhanced topographic wetness index (**b**), and the relief enhance topographic wetness index (**c**), LiDAR intensity during a dry (**d**) and average spring (**e**), and false color near-infrared aerial photograph (**f**; collected coincident to **e**) of a forested wetland complex within the study area. All images have been overlaid with a wetland map generated by the Maryland Department of Natural Resources. On the topographic index products, wetter areas are *blue* (more likely to be wetlands) while drier areas are *red* (less likely to be wetlands). Inundated areas are *black* on the LiDAR intensity images

LiDAR intensity based inundation maps were created using a simple thresholding technique that separated inundated and non-inundated areas (Lang and McCarty 2009). The LiDAR intensity threshold between inundated and non-inundated areas was determined using over one thousand ground-based control points collected coincident with the LiDAR intensity data collected for each date (see Lang and McCarty 2009 for further details). The topographic metric and inundation map comparison was an iterative process designed to test the products for different applications and compare the topographic metric based wetland maps to a related dataset, a wetland map based on aerial photography. First, all topographic metric based wetland maps were compared with the March 27, 2007 LiDAR intensity based inundation map to examine their ability to predict inundation patterns during average peak hydrologic expression (an indicator of wetland extent) since wetland maps are most frequently created to depict average conditions. Next, binary wetland-upland classified topographic metric based maps were compared with the March 27, 2007 LiDAR intensity based inundation map and an aerial photography derived wetland map to compare the relative ability of topographic metric and aerial photography derived wetland maps to predict inundation during peak hydrologic expression, an indicator of wetland extent. Finally, the March 24, 2009 LiDAR intensity based inundation map, as well as the March 27, 2007 LiDAR intensity based inundation map, were used to examine the ability of topographic metric based wetland maps to infer inundation under varying weather conditions. A more detailed description of these analysis steps can be found below.

All map products were compared with the March 27, 2007 LiDAR intensity derived map of inundation/non-inundation near average peak hydrologic expression that was found to be ~97 % accurate based on comparison with ground data (Lang and McCarty 2009). Since inundation status does not directly account for soil moisture (another physical manifestation of wetness), inundation status is not the same as wetland status and since the TWI maps are a continuous indicator of potential wetness and not a binary indicator of flooding for a particular date, the relationship between topographic metrics and the LiDAR intensity derived dataset will be referred to as predictive strength instead of accuracy.

A stratified random sampling approach was used to select over 2,000 reference points approximately evenly divided between inundated and non-inundated forest areas that were at least 10 m away from each other and 25 m away from the forest edge. Evergreen areas were avoided even though they represent a very small portion of the study area (<5 % of forested area or<.78 km^2) because reference data were likely be less reliable within these areas. This was accomplished using the 3 band visible/near-infrared digital image collected coincident with the March 2007 LiDAR data (Lang and McCarty 2009). Although much of the study area contains relatively shallow, hand dug ditches that were created in the early to mid – 1900s, a smaller portion of the study area contains deeper (>1.5 m) ditches that are currently maintained. Areas that were directly drained by these deeper ditches were identified and an all forest and non-drained forest reference dataset were created. The topographic metric values closest to each reference point were extracted using bilinear interpolation (vector data) or a spatial join (raster data).

The reference data were then used to compute percent reference points inundated or not inundated within each of the four (D8 TWI, D∞ TWI, FD8 TWI, LTNR, and ETWI) or seven (RETWI) topographic metric classes as an indication of predictive strength. Subsequently, the D8 and D∞ TWIs were excluded from further analysis (see results section). Percent of total forested area within the study site represented by each class (e.g., very likely to be upland) was then calculated for all topographic metric based wetland maps so that percent of total study area mapped with different levels of predictive strength could be computed. Total area of forest was determined using the 3 band visible/near-infrared digital image collected coincident with the March 2007 LiDAR data (Lang and McCarty 2009).

Each topographic metric based wetland map was then divided into binary wetland and upland classes to facilitate comparison with the MD DNR wetland map. For FD8 TWI, LTNR, and ETWI classes 1 and 2 (i.e., very likely to be upland and likely to be upland) were considered to be upland and classes 3 and 4 (i.e., likely to be wetland and very likely to be wetland) were considered to be wetland. Classes 2, 3, and 4 of the RETWI were considered to be upland while classes 5, 6, 7, and 8 were considered to be wetland. Although class 5 contained more non-inundated areas than inundated areas, it was considered a wetland class to better account for saturated areas. In theory, doing so operationally would produce a map with fewer omission errors. Percent reference points found to be inundated within wetlands and non-inundated within uplands were then calculated for each topographic metric based wetland map and the MD DNR wetland map. The binary wetland map based on the thresholded RETWI was overlaid on the MD DNR wetland map to determine degree of spatial agreement.

The LiDAR intensity image collected on March 24, 2009 was used to determine whether or not the existing non-ditched reference points were inundated during a spring of low water levels (i.e., drought). Approximately 6 % of the existing reference points (122 of 2000) were located at the transition between inundated and non-inundated areas on the 2009 inundation map and were therefore excluded from the analysis. The remaining 1,878 reference points were grouped into the following categories: 1) not inundated

during an average or drought spring (0 Y; 1000 points), 2) inundated only during an average spring (1 Y; 482 points), 3) inundated during average and drought springs (2 Y; 396 points), and 4) inundated during an average spring or inundated during an average and drought spring (1Y+2Y; 878 points).

Percent reference points within each of the four inundation categories were calculated for each class of the FD8 TWI, ETWI, LTNR, and RETWI topographic metrics. To normalize index values across all algorithms, the RETWI index was modified by dividing each index value by 2. A similar calculation was performed for MD DNR by dividing the wetland map into categories based on wetland status and hydroperiod as indicated by Cowardin classification (Cowardin et al. 1979) hydrologic modifier: 1) upland, 2) temporarily flooded wetlands, 3) seasonally flooded, 4) permanently flooded, semi-permanently flooded, and intermittently exposed wetlands. Categorizing the MD DNR polygons in this fashion places the map units in order from shortest to longest duration of inundation or saturation as indicated by wetland status and hydrologic modifier.

Statistical analyses were performed to assess the ability of the different topographic metric based wetland maps to discern inundation location and frequency as classified into the likelihood categories defined above (e.g., very likely to be wetland). In general, a larger significant difference in mean values across inundation categories was considered to be indicative of greater ability of the map to differentiate between categories. We treated data within each map as being interval data subject to parametric statistics to test if the differences in mean values for various categories were equal to zero (t test, P=< 0.1, 0.01, or 0.001). The category data were found to have non-normal distributions. However, according to central limit theorem (Snedecor and Cochran 1989) the sample means become normally distributed in sufficiently large populations with non-normal distribution of values. Sample populations analyzed in this study were large (n=396 to 1,000); therefore we used standard analysis.

Results

The ability of different topographic metric based wetland maps to differentiate between inundated and non-inundated areas varied between topographic metrics and map classes (Table 1). Of the three TWIs that were examined, the D8 TWI (99 % of pixels with D8 TWI values between 0 and 21) offered the least predictive strength. The D∞ (99 % of pixels with D∞ TWI values between 3 and 13) and FD8 (99 % of pixels with FD8 TWI values between 7 and 14) TWIs provided relatively similar levels of predictive strength (i.e., greatest ability to isolate inundated from non-inundated areas) but D∞ TWI map class boundaries appeared relatively

Table 1 Number and percent of reference points found to be inundated (Inun) or non-inundated (Not) for all classes of the enhanced TWI, local terrain normalized relief, relief enhanced TWI, D8 TWI, D∞ TWI, and FD8 TWI in all (no shading) or non-drained (bold) forests

Class	Inun	Not	%Inun	%Not
DEVELOPED TOPO METRICS				
Enhanced TWI				
1	0	117	0.0 %	100.0 %
2	7	529	1.3 %	98.7 %
3	314	355	46.9 %	53.1 %
4	698	19	97.4 %	2.6 %
1	**0**	**165**	**0.0 %**	**100.0 %**
2	**7**	**517**	**1.3 %**	**98.7 %**
3	**309**	**286**	**51.9 %**	**48.1 %**
4	**684**	**32**	**95.5 %**	**4.5 %**
Local Terrain Normalized Relief				
1	16	309	4.9 %	95.1 %
2	362	481	42.9 %	57.1 %
3	383	172	69.0 %	31.0 %
4	258	58	81.6 %	18.4 %
1	**17**	**423**	**3.9 %**	**96.1 %**
2	**354**	**466**	**43.2 %**	**56.8 %**
3	**380**	**98**	**79.5 %**	**20.5 %**
4	**249**	**13**	**95.0 %**	**5.0 %**
Relief Enhanced TWI				
2	0	71	0.0 %	100.0 %
3	0	216	0.0 %	100.0 %
4	15	297	4.8 %	95.2 %
5	114	300	27.5 %	72.5 %
6	367	100	78.6 %	21.4 %
7	347	31	91.8 %	8.2 %
8	176	5	97.2 %	2.8 %
2	**0**	**105**	**0.0 %**	**100.0 %**
3	**0**	**308**	**0.0 %**	**100.0 %**
4	**15**	**282**	**5.1 %**	**94.9 %**
5	**114**	**224**	**33.7 %**	**66.3 %**
6	**357**	**66**	**84.4 %**	**15.6 %**
7	**342**	**12**	**96.6 %**	**3.4 %**
8	**172**	**3**	**98.3 %**	**1.7 %**
ORIGINAL TOPO METRICS				
D8 TWI				
1	30	69	30.3 %	69.7 %
2	198	410	32.6 %	67.4 %
3	462	459	50.2 %	49.8 %
4	329	82	80.0 %	20.0 %
1	**29**	**76**	**27.6 %**	**72.4 %**
2	**199**	**461**	**30.2 %**	**69.8 %**
3	**453**	**395**	**53.4 %**	**46.6 %**
4	**319**	**68**	**82.4 %**	**17.6 %**
D∞ TWI				
1	0	125	0.0 %	100.0 %

Table 1 (continued)

Class	Inun	Not	%Inun	%Not
2	13	310	4.0 %	96.0 %
3	528	514	50.7 %	49.3 %
4	478	71	87.1 %	12.9 %
1	**0**	**155**	**0.0 %**	**100.0 %**
2	**13**	**347**	**3.6 %**	**96.4 %**
3	**520**	**430**	**54.7 %**	**45.3 %**
4	**467**	**68**	**87.3 %**	**12.7 %**
FD8 TWI				
1	0	98	0.0 %	100.0 %
2	79	472	14.3 %	85.7 %
3	426	375	53.2 %	46.8 %
4	514	75	87.3 %	12.7 %
1	**0**	**139**	**0.0 %**	**100.0 %**
2	**77**	**480**	**13.8 %**	**86.2 %**
3	**419**	**306**	**57.8 %**	**42.2 %**
4	**504**	**75**	**87.0 %**	**13.0 %**

artificial (i.e., narrow, linear) with the boundary between classes 3 and 4 being especially non-intuitive (extensive spurious linear features through flat areas; Fig. 5). Predictive strength of the FD8 TWI map was improved overall by increasing map values within areas without a surface water outlet to create the ETWI (99 % of pixels with ETWI values between 7 and 15; Table 1). Although all topographic metrics demonstrated some sensitivity to drainage as exhibited by differences in predictive strength as calculated using all forest (total area of 15.5 km^2 at study site) and only non-drained forest (total area of 11.4 km^2 at study site) reference datasets, LTNR (99 % of pixels with LTNR values between 0 and 6) was most sensitive to drainage condition. Predictive strength of LTNR class 4 (very likely wetland) increased ~14 % when only non-drained forests were considered. Particularly within non-drained forests, the LTNR performed well considering the simplicity of the index. Combining the ETWI and LTNR to create the RETWI further increased predictive strength. As expected, ETWI, LTNR, and RETWI map classes with the greatest predictive strength were those at either extreme of wetness condition (e.g., very likely to be upland or very likely to be wetland), although in general upland classes (e.g., 1 and 2) were mapped with greater certainty than wetland map classes (e.g., 3 and 4). The ETWI predicted inundation status over slightly less than 65 % of the forested landscape with predictive strength of over 95 % (Table 2). Although the RETWI mapped a smaller area than the ETWI at the 95 % performance level, it predicted inundation status over the entire forested landscape with a predictive strength of greater than 70 %. The area mapped with similar predictive strength by the FD8 TWI and LTNR maps was smaller.

The creation of binary wetland/upland maps based on topographic metrics allowed direct comparison with the MD DNR wetland map. Wetlands mapped using aerial photographs (MD DNR) and LiDAR derived DEMs (FD8 TWI, LTNR, ETWI, and RETWI) contained a similar amount of inundated area when the entire forested area was considered (Table 3). Understandably, percent inundation was higher for the topographic metric based maps when only non-drained forests were considered. The RETWI and ETWI mapped fewer (6–7 % all forests and non-drained forests) inundated areas as uplands than the MD DNR.

The MD DNR wetland map and RETWI binary wetland map agreed over approximately 65 % of the mapped area (Fig. 6). The MD DNR and RETWI wetland maps both mapped wetlands over 32 % of the total forest area (34 % non-drained forests) and both mapped uplands over 35 % of the total forest area (36 % non-drained forests). The MD DNR wetland map indicated wetlands while the RETWI binary wetland map indicated uplands over 11 % of the total forest area (12 % non-drained forests) and the RETWI binary map indicated wetlands while the MD DNR wetland

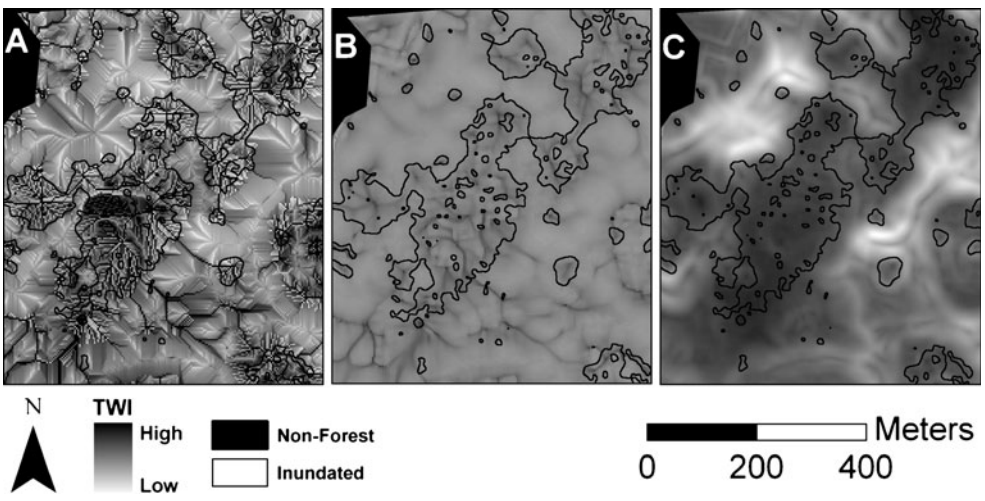

Fig. 5 Topographic wetness indices including those derived using the D8 (**a**), D∞ (**b**), and FD8 (**c**) flow routing algorithms overlaid with inundation boundaries from an average spring (March 2007) outlined in *black*. Non-forested areas are *solid black* and only appear in the northwest corner

Table 2 Percent study area correctly mapped as flooded or non-flooded at specified levels of predictive strength using the relief enhanced topographic wetness index (RETWI), enhanced topographic Wetness index (ETWI), FD8 TWI, and local terrain normalized relief (LTNR) maps for all forests (top) and only non-drained forests (below)

	Levels of predictive strength					
	≥70 %	≥75 %	≥80 %	≥85 %	≥90 %	≥95 %
Drained and Non-Drained Forests						
RETWI	100	70.1	53.8	53.8	53.8	47.59
ETWI	63.6	63.6	63.6	63.6	63.6	63.56
FD8 TWI	64.8	64.8	64.8	64.8	11.2	11.24
LTNR	29.8	29.8	29.8	21.7	21.7	21.71
Non-Drained Forests						
RETWI	71.7	71.7	71.7	55.9	55.8	55.9
ETWI	63.7	63.7	63.7	63.7	63.7	63.7
FD8 TWI	65.6	65.6	65.6	65.6	11.6	11.6
LTNR	53.0	53.0	53.0	31.7	31.7	31.7

map indicated uplands over 21 % of the total forest area (18 % non-drained forests). The RETWI map found 54 % of total forested area to be wetland while the MD DNR map found 44 % to be wetland.

A general trend of decreasing percent reference points not inundated either year (0 Y) and increasing percent reference points inundated both years (2 Y) was evident as classes increased from 1 to 4 (ETWI, LTNR, MD DNR) or 2 to 8 (RETWI; Fig. 7). Statistical analysis of the differences in mean values generated by the topographic algorithms across four categories of inundation (Table 4) showed that all metrics produced statistically significant differences in mean values when differentiating non-inundated locations (0 Y) from locations subject to 1 or 2 years inundation (i.e., 0 Y vs. 2 Y; 0 Y vs. 2 Y; 0 Y vs. 1 Y+2 Y). The maps based primarily on topographic wetness indices (FD8 TWI and ETWI) did not produce significant mean differences for the category differentiating locations with 1 year and 2 years inundation (1 Y vs. 2 Y) but the indices that included local relief (LTNR and RETWI) produced significant differences for this category.

Table 3 Percent wetland class found to be inundated and upland class found to be non-inundated. Upland areas that are flooded are likely to be wetland errors of omission. Wetland areas that are not flooded may still be saturated within the root zone and considered to be wetlands. Therefore predictive strength is likely to be higher than indicated by percent wetland area inundated and the difference between these values and one hundred do not simply represent errors of commission. It is notable that RETWI and ETWI contain fewer hypothetical upland errors of commission than MD DNR and all maps contain similar percentages of wetland classes that are inundated

	All forest		Non-drained forest	
	% Wet	% Up	% Wet	% Up
RETWI	69.7	97.5	76.3	97.9
ETWI	73.0	98.9	75.7	99.0
LTNR	73.6	67.7	85.0	70.6
FD8 TWI	67.6	87.8	70.8	88.9
MD DNR	72.0	91.6	72.8	92.1

Discussion

Although inundation status is not the same as wetland status, areas that are inundated just prior to the growing season are very likely to meet the hydrologic definition of a wetland (i.e., inundated or saturated in the root zone for 2 weeks within the growing season). On the other hand, areas that are not inundated at this time may still meet the hydrologic definition of a wetland but the majority of these areas are not likely to do so in this landscape. Therefore the use of the reference data described above provides a conservative estimate of wetland location and results should be judged within this context. However, LiDAR intensity data have been found to map inundation approximately 30 % more accurately than 1 m false color near-infrared aerial photographs at this study site (Lang and McCarty 2009; results based on ground data). Therefore this method is a significant improvement upon using aerial photographs to infer accuracy, and provides many more reference points than is practical using ground-based wetland delineation.

A number of flow routing algorithms have been proposed to best suit different needs and applications. Although none appear to be ideal for all applications (Arnold 2010; Kopecky and Cizkova 2010), the results of this paper support the use of more distributed (multiple flow direction; e.g., FD8) flow routing algorithms over algorithms that encourage greater flow convergence (e.g., D8 and D∞) for the mapping of forested palustrine wetlands. Evidence of varying levels of flow convergence between flow routing algorithms is provided by the different ranges of pixel values within TWIs based on different flow routing algorithms (i.e., greater range indicates greater convergence).

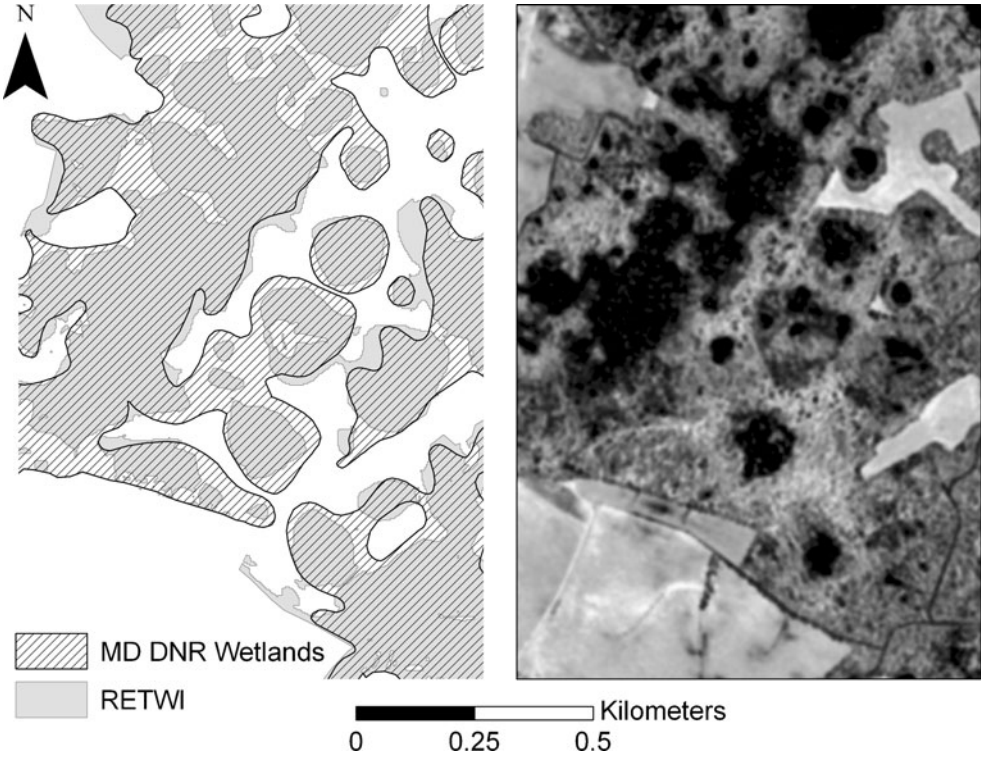

Fig. 6 Map showing the spatial relationship between MD DNR and RETWI wetland maps for one location within the study area (*left*) and an average spring LiDAR intensity image for the same area (*right*)

The use of multiple flow direction algorithms to best characterize gradual ecologic transitions based on soil moisture gradients has been endorsed by other studies (Wolock and McCabe 1995; Kopecky and Cizkova 2010), especially on hill slopes (Quinn et al. 1991). This may be especially true in areas of low topographic relief where slopes are more gradual and flow is less channelized. Conversely, the use of algorithms with greater flow convergence (e.g., D8 and D∞) has been suggested for applications involving the mapping of flow channels (Tarboton 1997; Bohner et al. 2001) and watershed boundaries (Arnold 2010). These algorithms tend to represent the distribution of flow (wetness) as narrow, linear pathways (Arnold 2010; Quinn et al. 1991; Wolock and McCabe 1995) instead of the smoother, broader wet zones that are more typical of wetland distribution. These trends were clearly evident when visually comparing TWIs based on different flow routing algorithms at our study site (Fig. 5).

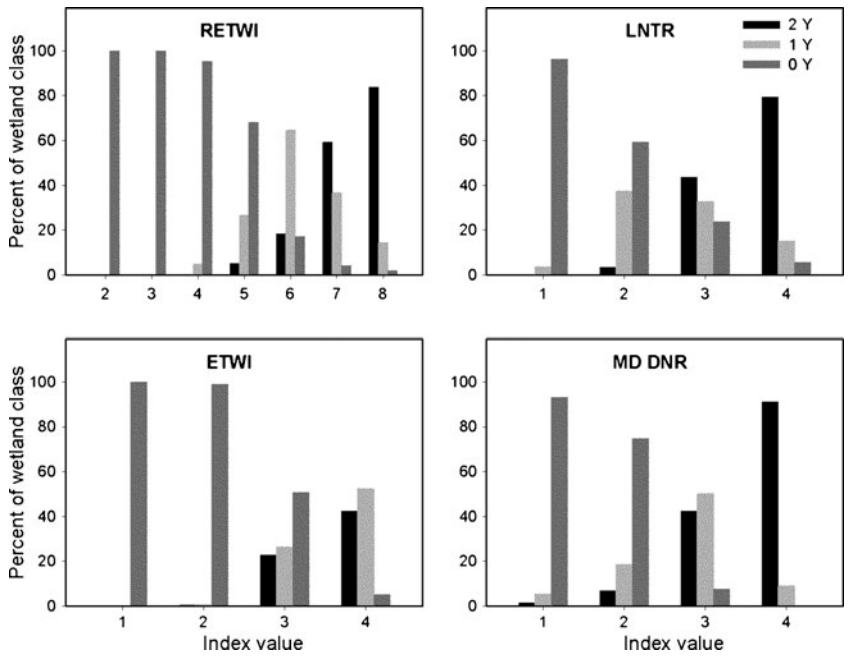

Fig. 7 Percent of wetland map classes found to be flooded during both average and dry years (2 Y), only average years (1 Y), and neither average or dry years (0 Y) for the relief enhanced topographic wetness index (RETWI; *top left*), the enhanced topographic wetness index (ETWI; *bottom left*), local terrain normalized relief (LTNR; *top right*), and the Maryland Department of Natural Resources wetland map (MD DNR; *bottom right*). Lower classes (*horizontal axis*) are more likely to be uplands while higher classes are more likely to be wetlands

Table 4 Differences in mean index values generated by topographic metrics across four classes of inundation in a population of randomly stratified sampling locations (n=1,878). The inundation class for each location was evaluated using LiDAR intensity derived inundation maps acquired in March 2007 (average weather) and 2009 (drought). The sample population included 1,000 locations with no inundation for both years (0 Y), 482 locations with 1 year inundation (1 Y), 396 locations with 2 years inundation (2 Y) and combined 878 locations with 1 or 2 years inundation (1 Y+2 Y)

Metric	Difference in mean index values across indicated inundation classes			
	1 Y vs. 0 Y	2 Y vs. 0 Y	1 Y vs. 2 Y	1 Y+2 Y vs. 0 Y
FD8 TWI	1.14***	1.04***	0.10*	1.10***
ETWI	1.49***	1.48***	0.01	1.49***
LTNR	0.70***	1.71***	1.01***	1.15***
RETWI[a]	1.03***	1.56***	0.54***	1.05***

*, **, and *** t-test results indicating difference in mean values was significantly different from zero at P=<0.1, 0.01, and 0.001, respectively

[a] to normalize index values across all algorithms, the RETWI index was modified by dividing each index value by 2

It is hypothesized that the enhancement of the FD8 algorithm through the incorporation of information on surface water flow outlets to create the ETWI map more completely represented the output of surface water (i.e., presence of surface water outlets) from a given area to compliment the input of surface water (i.e., specific catchment area). By definition, a pit or sink is an area of one or more pixels that is surrounded by areas of higher elevation so that flow direction cannot be assigned. Therefore, areas that are pits/sinks do not have a surface water outlet. In areas of low topographic relief and numerous depressions, it is likely that slope is less indicative of water leaving the target area. Grabs et al. (2009) state that in areas of low topographic relief, slope can overestimate the downslope hydraulic gradient due to the presence of downslope water tables. This may partially explain why the addition of information on the presence or absence of surface water outlets, which helps to better determine the ability of water to exit an area, was helpful.

Information on flow outlets was incorporated into the mapping process by increasing FD8 TWI values in pits or closed depressions. In many applications of flow routing, these closed depressions are filled before flow is routed across the landscape to avoid trapping flow within these depressions, most of which were traditionally considered to be errors in the DEM (Arnold 2010). However, filling these depressions may not be advisable when mapping water accumulation in areas with depressional wetlands. Methods have been proposed to prevent filling wetland depressions (Gritzner 2006), but these methods depend on an accurate wetland map, which is often not available, especially in forested areas. Furthermore, the quality of LiDAR based DEMs has improved significantly since the filling of pits was originally recommended as a standard protocol, making this technique less desirable in general (Arnold 2010). Running flow routing algorithms without filling pits can lead to unwanted map artifacts (Fig. 5), which were present in the D8 derived TWI but not the FD8 TWI.

Differences in the mean index values generated by the map products across classes of inundation (i.e., 0 Y, 1 Y and 2 Y) help to quantify the ability of different algorithms to determine wetland boundaries and temporal fluctuations in inundation (Table 4). The results of statistical analysis indicate that both FD8 TWI and ETWI algorithms were relatively good at mapping locations with high potential for inundation during relatively wet periods (i.e., average spring) but the TWIs had very limited ability to predict frequency of inundation accounting for drier periods (1 Y versus 2 Y; Table 4 and Fig. 7). By contrast LTNR performed best for distinguishing areas with expected water accumulation during drier periods thus better explaining frequency of inundation through time but was least able to predict the extent of water accumulation during an average spring. As may be expected, the hybrid RETWI algorithm gained traits of both ETWI and LTNR and was able to both map wetland location and predict inundation frequency through time accounting for drought. Grayson et al. (1997) hypothesized that lateral controls (e.g., contributing area) are most likely to be good predictors of water accumulation during wet periods and that more local controls (e.g., surface curvature) tend to control water accumulation during drier periods. Our findings regarding the relatively poor suitability of TWI based metrics during a time of drought relative to a wetter period support this theory. Furthermore, LTNR represents a vertical control on water accumulation and as predicted by Grayson et al. (1997), it was better adapted to the mapping of inundation during a drier period. To compensate for the limitations of TWI during dry conditions, Grayson et al. (1997) advocate the use of multiple metrics to account for both lateral and vertical flow, as implemented in this study.

The ability of LTNR to predict areas of inundation during periods of less than average precipitation significantly adds

to the types of applications that can be addressed by the topographic metrics detailed in this paper. For example, these areas may provide vital biodiversity support through the provision of amphibian habitat (i.e., refugia) during drought years. This finding is relevant to the development of climate change adaptation strategies since models predict that periods of drought and/or flood will become more common in the Mid-Atlantic (Mid-Atlantic Regional Assessment Team 2000). The ability of LTNR to predict weather driven changes in inundation (i.e., drought) may also be indicative of its ability to predict intra-annual fluctuations in hydroperiod since groundwater level is a primary driver of both inter- and intra-annual fluctuations in water levels at this study site. The similarity of the temporal patterns discerned using the LTNR and MD DNR wetland maps categorized by hydrologic modifier and the sensitivity of the LTNR product to ditching which generally lowers groundwater levels, supports this assertion (Fig. 7). It is therefore hypothesized that the LTNR map could be used to map hydroperiod at the study site, similarly to existing wetland maps (e.g., NWI). This assertion should be tested more rigorously through subsequent studies.

The ETWI and LTNR maps were combined due to their sensitivity to two relatively unique drivers of wetland hydrology. The ETWI depicts changes in water distribution across the landscape based on lateral inflows and outflows. We hypothesize that the LTNR depicts variations due, at least in part, to the surface expression of groundwater since in Coastal Plain areas with a surficial aquifer wetlands with greater relief as judged relative to a small area (e.g., 200 m^2) are more likely to encounter shallow groundwater (Winter 1988). The concentration of water within low areas as inundation recedes is also a likely contributor to the predictive power of LTNR. By combining the two metrics, areas that are more likely to support wetland hydrology through both mechanisms (i.e., lateral and vertical movement of water) can be identified while areas that could support wetland hydrology through only one mechanism are deemphasized (Fig. 4).

Just as certain levels of wetness are considered to define wetland boundaries, the continuous topographic metrics were thresholded to indicate the probability of wetland presence. Thresholding the topographic metrics served four purposes: 1) to allow for the incorporation of professional judgment and the tailoring of the topographic metrics to different landscapes; 2) to create a classified map product that would be easier to incorporate into current natural resource management operational activities that are adapted to a binary mapping system; 3) to ease the comparison of the LiDAR derived map products with currently available products (i.e., MD DNR); and 4) to facilitate the combining of different maps (e.g., LTNR and ETWI) to produce enhanced end products. However, since a sensitivity analysis was not performed as part of the thresholding process, it is possible that the selected thresholds affected the relative performance of the different indices. Different thresholds should be set based on the drivers of water distribution at individual study sites and the goal of the mapping exercise. A sensitivity analysis could help optimize threshold selection.

The topographic metrics and the methods described in this paper should not be assumed to provide the same value in all landscapes. For example, these metrics should be applied with caution in areas with insignificant topographic relief, where groundwater interactions cannot be reasonably predicted using topographic metrics, with highly permeable soils where vertical movement of water will dominate lateral movement of water, and that have been highly engineered to modify water distribution across the landscape. These metrics provide the operational wetland mapper with some degree of flexibility to best represent wetland distribution and boundaries within different study sites. In areas where lateral redistribution of water is the dominant control on the formation of wetlands and expression of groundwater is less so (e.g., areas with a confining soil layer), the use of TWIs could be emphasized over relief. In addition, the operational wetland mapper could decide whether to use the topographic metrics as a guide while manually delineating boundaries or to automatically incorporate topographic metric based classes with acceptable levels of certainty (Table 2). More research is needed to test the applicability of the topographic metrics described in this paper to other areas and to determine the best way to incorporate topographic metric data into operational wetland mapping. However, the strong performance of these metrics in an area of relatively low topographic relief is promising since it is generally considered to be difficult to determine flow paths in these areas (Wilson et al. 2007).

Spatial scale (i.e., resolution) and map extent should be appropriate to the primary drivers of water distribution across the landscape. For this reason, care should be taken to match the resolution of input DEMs to the size of topographic variations leading to differences in water accumulation pertinent to the formation of wetlands. Although LiDAR sensors are capable of producing extremely fine resolution DEMs (e.g., < 0.5 m pixels), it is not always advantageous to use such fine resolution datasets to map wetlands. Similarly, coarse resolution DEMs (50 m) have been found to not be ideal for the mapping of wetlands (Rohde and Seibert 1999). The resampling and filtering performed as part of this analysis served the dual function of reducing possible DEM errors and decreasing microtopography that could lead to unduly complicated and unrealistic wetland boundaries. Care should be taken to limit the extent of analysis to landscapes with similar uncompensated controls on distribution of inundation and near surface soil saturation (e.g., weather). For this reason and due to the

varying quality of DEMs across political boundaries (e.g., states), the application of a uniform topographic metric to regional and larger scales is not recommended (Kopecky and Cizkova 2010). Instead, tailoring topographic metrics to more local areas should increase their predictive power. Additional research is necessary to discern the most advantageous indices and appropriate spatial scales for use in different landscapes.

It should be noted that accuracy of topographic metrics, such as TWIs, is largely dependent on the accuracy and spatial resolution of the input DEM. Furthermore, LiDAR data should be collected to different specifications based on their intended application and data collected for one application may not be suitable for another. For example, vegetation cover is known to reduce bare earth LiDAR resolution but bare earth spatial resolution (i.e., point density) can be optimized in forests by collecting LiDAR data during the leaf-off phenological period and modifying sensor parameters (e.g., decreasing scan angle). When using LiDAR based DEMs to map wetlands it is important not only that the DEM be relatively free of errors, but that inundation not have been present during LiDAR collection since the presence of an inundated surface is likely to decrease returns from the inundated area and raise bare earth elevation above the true land surface. Both the presence of a vegetative canopy, especially a leaf-on canopy, and inundation will also reduce vertical accuracy (Hogg and Holland 2008). For this reason LiDAR data were collected during the leaf-off season when forested wetlands in the study area were generally not inundated. However, decreased vertical accuracy within forested areas relative to open areas is still likely (Hodgson and Bresnahan 2004; 26 cm RMSE) but it should be noted that even with this decrease in accuracy, LiDAR derived DEMS are still much more accurate than non-LiDAR derived DEMs (1 – 10 m). If necessary, this reduction in accuracy could be quantified using a dual GPS and total station approach (Hodgson and Bresnahan 2004).

Conclusions

We demonstrated that the predictive power and efficiency of wetland mapping efforts could be improved through the incorporation of LiDAR derived DEMs into the wetland mapping process. This advancement should be supported by increasing LiDAR data availability and consistency, more robust and accessible software processing capabilities, further development of applications, and increased integration of LiDAR data into the operational geospatial data-processing chain. The use of LiDAR data will be especially vital in areas with low topographic variation or when applied to mapping or monitoring wetlands that have previously been difficult to detect, such as forested wetlands.

Steps are currently being taken by the NWI (personal communication Ralph Tiner, US Fish and Wildlife Service, 2011) and other environmental resource agencies (Hogg and Holland 2008) to investigate the integration of LiDAR data into the operational wetland mapping process. Optical (e.g., aerial photography) and LiDAR data are distinct remotely sensed datasets which offer unique benefits and limitations. The synergistic combination of these datasets has the potential to significantly improve the mapping of forested wetlands which are difficult to map using optical data alone and extremely time consuming to map from the ground.

Acknowledgments This research was supported by the wetland component of the Natural Resources Conservation Service Conservation Effects Assessment Project. We greatly acknowledge the cooperation of private landowners, especially The Nature Conservancy. All trade names are included for the benefit of the reader and do not imply an endorsement of or preference for the product listed by the U.S. Department of Agriculture. USDA is an equal opportunity provider and employer.

References

Arnold N (2010) A new approach for dealing with depressions in digital elevation models when calculating flow accumulation values. Prog Phys Geogr 34:781–809

Ator SW, Denver JM, Krantz DE, Newell WL, Martucci SK (2005) A surficial hydrogeologic framework for the Mid-Atlantic Coastal Plain. U.S. Department of the Interior. Professional Paper 1680

Beven K, Kirkby M (1979) A physically based variable contributing area model of basin hydrogy. Hydrol Sci Bull 24:43–69

Bohner J, Kothe R, Conrad O, Gross J, Ringeler A, Selige T (2001) Soil regionalisation by means of terrain analysis and process parameterisation. Eur Soil Bur :213–222

Bohner J, Selige T (2006) Spatial prediction of soil attributes using terrain analysis and climate regionalisation. In: Bohner J, McCLoy KR, Strobl J (eds) Gottinger Geographische Abhandlungen 115:13–28

Chust G, Galparsoro I, Borja A, Franco J, Uriarte A (2008) Coastal and estuarine habitat mapping using lidar height and intensity and multi-spectral imagery. Estuarine Coastal Shelf Sci 78:633–643

Conrad O (2006) SAGA - program structure and current state of implementation. In: Bohner J, McCLoy KR, Strobl J (eds) Gottinger Geographische Abhandlungen 115:39–52

Coren F, Sterzai P (2006) Radiometric correction in laser scanning. Int J Remote Sens 27:3097–3104

Cowardin LM, Carter V, Golet F, LaRoe E (1979) Classification of wetlands and deepwater habitats of the United States. U.S. Fish and Wildlife Service, Washington, DC. FWS/OBS-79/31

Curie F, Gaillard S, Ducharne A, Bendjoudi H (2007) Geomorphological methods to characterise wetlands at the scale of the Seine Watershed. Sci Total Environ 375:59–68

Freeman TG (1991) Calculating catchment-area with divergent flow based on a regular grid. Comput Geosci 17:413–422

Grabs T, Seibert J, Bishop K, Laudon H (2009) Modeling spatial patterns of saturated areas: a comparison of the topographic wetness index and a dynamic distributed model. J Hydrol 373:15–23

Grayson RB, Western AW, Chiew FHS, Bloschl G (1997) Preferred states in spatial soil moisture patterns: local and nonlocal controls. Water Resour Res 33:2897–2908

Gritzner JH (2006) Identifying wetland depressions in bare-ground lidar for hydrologic modeling. ERSI user conference proceedings 2006. http://proceedings.esri.com/library/userconf/proc06/papers/papers/pap_1225.pdf. Accessed 12 Sept 2006

Hodgson ME, Bresnahan P (2004) Accuracy of airborne lidar derived elevation: empirical assessment and error budget. Photogramm Eng Remote Sens 70:331–339

Hogg AR, Holland J (2008) An evaluation of DEMs derived from lidar and photogrammetry for wetland mapping. For Chron 84:840–849

Kopecky M, Cizkova S (2010) Using topographic wetness index in vegetation ecology: does the algorithm matter? Appl Veg Sci 13:450–459

Kudray GM, Gale MR (2000) Evaluation of national wetland inventory maps in a heavily forested region in the upper Great Lakes. Wetlands 20:581–587

Lang MW, McCarty GW (2009) Lidar intensity for improved detection of inundation below the forest canopy. Wetlands 29:1166–1178

Lefsky MA, Cohen WB, Parker GG, Harding DJ (2002) Lidar remote sensing for ecosystem studies. Bioscience 52:19–30

Lopes A, Touzi R, Nezry E (1990) Adaptive speckle filters and scene heterogeneity. IEEE Trans Geosci Remote Sens 28:992–1000

McCarty GW, McConnell LL, Hapernan CJ, Sadeghi A, Graff C, Hively WD, Lang MW, Fisher TR, Jordan T, Rice CP, Codling EE, Whitall D, Lynn A, Keppler J, Fogel ML (2008) Water quality and conservation practice effects in the Choptank River Watershed. J Soil Water Conserv 63:461–474

Mid-Atlantic Regional Assessment Team (2000) Preparing for a changing climate: the potential consequences of climate variability and change. Environmental Protection Agency and Pennsylvania State University, U.S

Moore ID, Grayson RB, Ladson AR (1991) Digital terrain modeling - a review of hydrological, geomorphological, and biological applications. Hydrol Processes 5:3–30

Murphy PNC, Ogilvie J, Arp P (2009) Topographic modeling of soil moisture conditions: a comparison and verification of two models. Eur J Soil Sci 60:94–109

O'Callaghan JF, Mark DM (1984) The extraction of drainage networks from digital elevation data. Comp Vision Graph Image Process 28:323–344

Quinn P, Beven K, Chevallier P, Planchon O (1991) The prediction of hillslope flow paths for distributed hydrological modelling using digital terrain models. Hydrol Processes 5:59–79

Rohde A, Seibert J (1999) Wetland occurrence in relation to topography: a test of topographic indices as moisture indicators. Agric For Meteorol 98–99:325–340

Snedecor GW, Cochran WG (1989) Statistical methods, 8th edn. Blackwell Publishing, Ames

Sorensen R, Zinko U, Seibert J (2006) On the calculation of the topographic wetness index: evaluation of different methods based on field observations. Hydrol Earth Syst Sci 10:101–112

Stolt MH, Baker JC (1995) Evaluation of national wetland inventory maps to inventory wetlands in the southern Blue Ridge of Virginia. Wetlands 15:346–353

Tarboton DG (1997) A new method for the determination of flow directions and upslope areas in grid digital elevation models. Water Resour Res 33:309–319

Tiner RW (1990) Use of high-altitude aerial-photography for inventorying forested wetlands in the United States. For Ecol Manag 33–4:593–604

Vierling KT, Vierling LA, Gould WA, Martinuzzi S, Clawges RM (2008) Lidar: shedding new light on habitat characterization and modeling. Front Ecol Environ 6:90–98

Walker CM, King RS, Whigham DF, Baird SJ (2012) Landscape and wetland influences on headwater stream chemistry in the Kenai Lowlands, Alaska. Wetlands 32:301–310

Wilson JP, Lam CS, Deng YX (2007) Comparison of the performance of flow-routing algorithms used in gis-based hydrologic analysis. Hydrol Processes 21:1026–1044

Winter TC (1988) A conceptual framework for assessing cumulative impacts on the hydrology of nontidal wetlands. Environ Manag 12:605–620

Wolock DM, McCabe GJ (1995) Comparison of single and multiple flow direction algorithms for computing topographic parameters in TOPMODEL. Water Resour Res 31:1315–1324

Yu K, Han S-H, Chang H, Ha T-J (2002) Potential of reflected intensity of airborne laser scanning systems in roadway features identification. Geomatica 56:363–374